STScI | SPACE TELESCOPE SCIENCE INSTITUTE

Instrument Science Report WFC3 2022-08

WFC3/UVIS Gain Stability Results for Cycles 26 - 29

K. Huynh & B. Kuhn

November 21, 2022

Abstract

We present new WFC3 UVIS CCD absolute gain measurements for December 2018 (Cycle 26) through June 2022 (Cycle 29). We employ the mean-variance technique using internal flat field image pairs taken in unbinned, 2×2, and 3×3 binned modes. As in previous programs, there are two epochs of data per Cycle, one in December and a second in June the following year. We find that the final gain values for the latest June 2022 unbinned data are 1.587 ± 0.007, 1.578 ± 0.004, 1.607 ± 0.005, 1.592 ± 0.006 e-/DN for amps A, B, C, and D respectively. In addition to analyzing the newest Cycles, we also looked at the full evolution of gain measurements over time. We find that while the gain measurement continues to increase Cycle to Cycle, it remains stable and consistent within 1-2% of past Cycles and the initial TV3 (ground) testing. We also investigate charge transfer efficiency (CTE) effects, and determine that increasing gain measurements is partially attributed to CTE degradation.

Introduction

CCD gain is defined as the number of electrons needed to register one count, or data number (DN), on the detector. A steady absolute gain value is an indicator that the WFC3 UVIS detectors are in healthy condition. Any large fluctuations in gain measurements over time will affect other measurements such as read-noise and photometric zeropoints (Gunning 2015) and would be an indication of possible changes in the electronic signal chain of the CCD (Martlin 2016). The UVIS gain is measured using the standard mean-variance technique on

back to back flat field image pairs, such that the gain is equal to the inverse slope of the fitted line to the variance vs mean signal for each amplifier (Baggett 2008).

In this work, we calculate the gain of the UVIS detector in unbinned mode with and without charge transfer efficiency (CTE) correction, as well as 2×2, and 3×3 binned modes. This report encapsulates the procedures used to make the gain measurements and the results for each of the two epochs in Cycles 26 - 29.

Data

Just like in previous Cycles, CCD gain data for Cycles 26 - 29 (Program IDs 15574, 15719, 16399, 16571) consist of internal flat field image pairs taken through the F645N filter using the default tungsten lamp at exposure times ranging from 0.48 to 105.0 seconds and three different binning modes: unbinned 1×1, 2×2, and 3×3. A 60 second exposure is taken at the beginning of each visit to warm up the tungsten lamp. Therefore, the gain cannot be properly assessed in this 60 second variable exposure and are excluded from the analysis. UVIS gain stability data for Cycles 26 - 29 are taken in two epochs, the first in December and the second in June of the following year. Table 2 located in the Appendix lists proposal IDs, Cycle numbers, epochs, and binning data distribution for each of the gain measurement datasets.

Analysis

WFC3/UVIS gain analysis for Cycles 26 - 29 is done with an automated pipeline written in 2015 that has been updated to remove IRAF dependencies (Fowler 2018). The pipeline calculates the gain in each amp through these steps:

1. Obtain exposure pairs and sort them by binning and exposure time.

2. Run `calwf3`, the automated calibration pipeline that reduces WFC3 images, on every exposure with a custom cosmic ray rejection table with values **SKYSUB** = mean, **CRRADIUS** = 2.1, **CRTHRESH** = 0.5555, **CRSIGMAS** = [6.5 , 5.5, 4.5], and **SCALENSE** = 3.0.

3. Flag bad pixels in the science array using all non-zero flags in the data quality array such as bad pixel columns, hot pixels, and cosmic rays, among others.

4. Calculate average and difference images from each exposure pairs.

5. Slice each image into square regions that vary depending on the binning: thirteen 200×200 slices for unbinned, nine 100×100 slices for 2×2, and ten 66×66 slices for 3×3 binned mode. The number and sizes of slices is tuned to each bin product to sample the full image with equal size pieces.

6. Verify the mean is $< 30{,}000$ DN and at least 85 % of the pixels are good (i.e not masked) in each square region. Square regions that fail to meet these conditions are discarded and not used in the analysis.

7. Calculate the mean and variance across the square slices for each image. Binned data is clipped at the 3 sigma level with 3 iterations, while no clipping is performed on unbinned data.

8. Plot the final variance as a function of mean signal for each amp and binning mode. A weighted 1st degree polynomial is then fit to the data and the gain value is determined by computing the inverse of the slope.

We made syntactical modifications to the pipeline in order for it to work with newer Python packages and run on older gain stability programs. We also added a new functionality that checks the HST Calibration Reference Data System (CRDS) and updates the best reference files and tables for every image before calibration. Finally, the pipeline now calculates the uncertainty of the absolute gain measurements through error propagation of the weighted line of best fit to the mean-variance data. With these modifications, we recalculated all past on-orbit gain programs from October 2009 to June 2018 (Cycles 17 - 25) under a single version of the pipeline for uniformity. We attempted to process thermal-vacuum (TV3) ground testing data from 2008, however we ran into issues running `calwf3` on the ground data and failed to obtain new gain measurements and uncertainties with the updated pipeline for TV3 testing. As a result, we use previously published gain measurements and uncertainties for thermal-vacuum ground testing. Gain measurements made with the updated version of the pipeline were within 5% of previously published values. This difference can be attributed to things such as Python package updates, algorithm changes, different reference files and tables, updates to calwf3, and machine precision.

Results

The variance vs mean signal plots for each amp in the unbinned mode for Cycle 29 are presented in Figure 1. The variance vs mean signal plots for 2x2 and 3x3 binned modes are presented in Figures 4 - 6 in the Appendix.

Figure 2 shows CCD gain stability data for each amp from October 2009 to June 2022 (Cycles 17 - 29). Table 1 shows the full history of CCD gain stability data calculated using the updated gain calibration pipeline for the unbinned case. Much like previous Cycles, newer gain data from December 2018 to June 2022 exhibit a <1% increase in gain suggesting a drift in the detector behavior over time, however the gain values still remain stable and within 1-2% of the initial thermal-vacuum (TV3) ground testing values in 2008. There are small dips in gain values that are consistent with all 4 amps in June of 2014, 2017, and 2021 (Cycles 21, 24, ad 28 respectively). Furthermore, there are low gain measurements at the end of 2009 and early 2010 in amps B and C, as well as higher gain measurements in amp B from 2011 - 2013. No apparent cause can be determined for the identified dips and rise in those gain measurements, however all of the excursions are within the error bars.

The increase in gain measurements over time appears to be at least partially due to CTE effects. CTE is a measure of how well charge packets are transferred pixel-by-pixel down the detector to the readout amplifier. The UVIS detector receives radiation damage in space, and one of the consequences is an increase in the number of charge traps over time, which results in flux loss. Due to the way the UVIS detector is read out, the charge packets

contained in the pixels closest to the chip gap (the bottom of UVIS1 and the top of UVIS2) experience the most number of transfers, and thus encounter the most amount of charge traps on their way to the read out amplifiers. This results in a greater flux loss for pixels further away from the amplifiers.

To observe the effects of CTE losses on the gain measurements, we split the CCD into two halves horizontally, where one half was closer to the amplifiers and the other was further from the amplifiers. The gain stability analysis was then run on each half separately in the same manner as the full CCD to calculate the absolute gain (as detailed in the Analysis section). Figure 3 presents the evolution of gain measurements for the two CCD halves over plotted with the previously shown full CCD gain measurements in Figure 2.

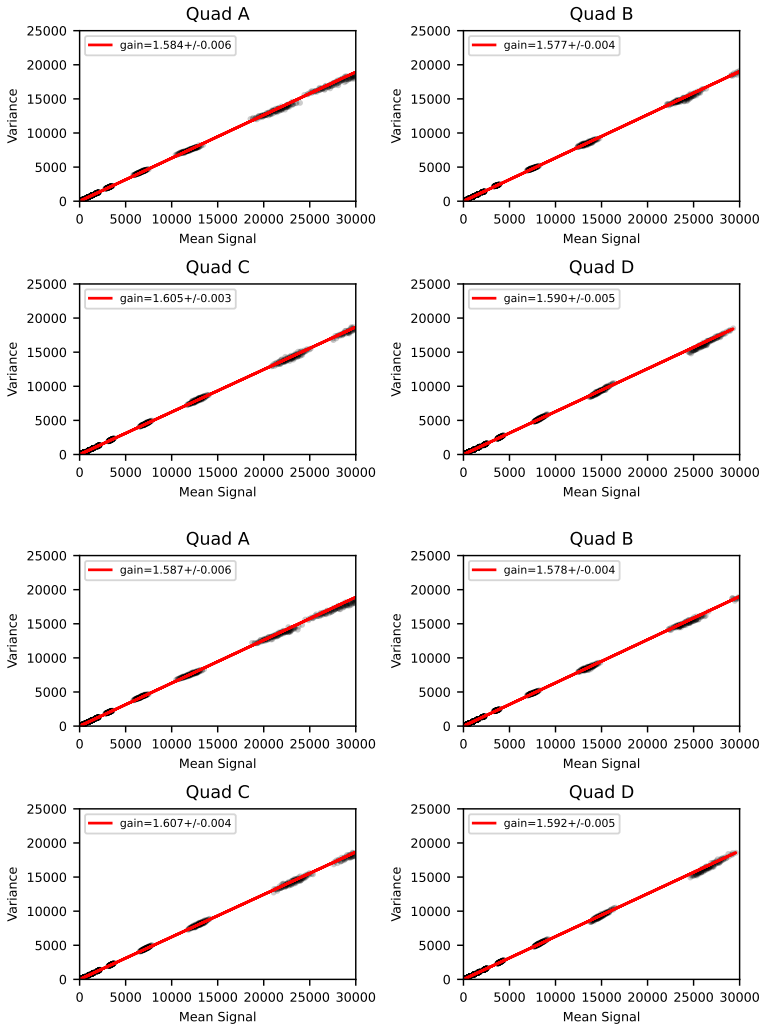

Figure 1: *Mean-variance plots for Cycle 29 unbinned non-CTE corrected images for Epoch 1 (Top) and Epoch 2 (Bottom) where the mean is in units of DN and the variance is in units of DN^2. The fitted slope is over plotted in red and the gain listed in the legend is the inverse slope. Each point in the plots represents the mean-variance for a square region of the detector.*

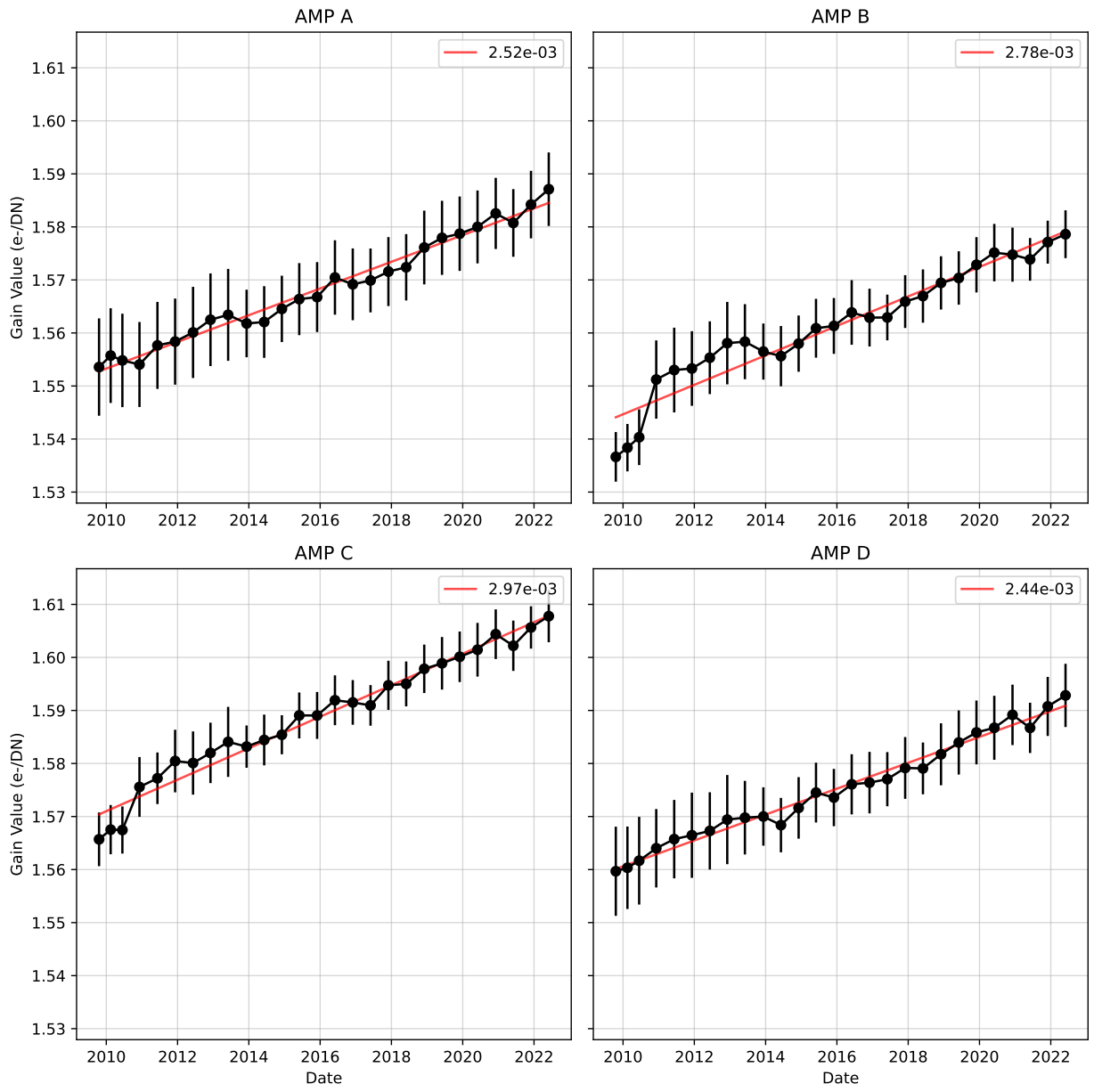

Figure 2: *Gain stability measurements across all four amplifiers for all unbinned on-orbit data from October 2009 to June 2022. The uncertainties are calculated through error propagation of the weighted line of best fit to the mean-variance data (i.e. Figure 1). A weighted 1st degree polynomial is fitted to the data and the slope is displayed to convey the change in absolute gain over time. Gain measurements taken in June 2014, June 2017, and June 2021 (Cycles 21, 24, and 28) exhibit a dip across all detectors. In Amps B and C, there are relatively low gain values from late 2009 to early 2010. There are also relatively high gain values in Amp B from 2011 - 2013. Despite these excursions, they all remain within the error bars.*

Table 1: *CCD gain results, in e-/DN, and associated errors since TV3 (ground) testing for unbinned data. Apart from TV3, every value is calculated using the same software and modified analysis.*

Cycle and Epoch	Amp A	Amp B	Amp C	Amp D
TV3	1.560 +/- <0.01	1.560 +/- <0.01	1.580 +/- <0.01	1.570 +/- <0.01
SMOV	1.561 +/- 0.011	1.559 +/- 0.011	1.583 +/- 0.009	1.582 +/- 0.014
Cycle 17 E1	1.553 +/- 0.009	1.536 +/- 0.004	1.565 +/- 0.005	1.559 +/- 0.008
Cycle 17 E2	1.555 +/- 0.008	1.538 +/- 0.004	1.567 +/- 0.004	1.560 +/- 0.007
Cycle 17 E3	1.554 +/- 0.008	1.540 +/- 0.005	1.567 +/- 0.004	1.561 +/- 0.008
Cycle 18 E1	1.554 +/- 0.008	1.551 +/- 0.007	1.575 +/- 0.005	1.564 +/- 0.007
Cycle 18 E2	1.557 +/- 0.008	1.553 +/- 0.007	1.577 +/- 0.004	1.565 +/- 0.007
Cycle 19 E1	1.558 +/- 0.008	1.553 +/- 0.007	1.580 +/- 0.005	1.566 +/- 0.008
Cycle 19 E2	1.560 +/- 0.008	1.555 +/- 0.006	1.580 +/- 0.005	1.567 +/- 0.007
Cycle 20 E1	1.562 +/- 0.008	1.558 +/- 0.007	1.581 +/- 0.005	1.569 +/- 0.008
Cycle 20 E2	1.563 +/- 0.008	1.558 +/- 0.007	1.584 +/- 0.006	1.569 +/- 0.006
Cycle 21 E1	1.561 +/- 0.006	1.556 +/- 0.005	1.583 +/- 0.003	1.570 +/- 0.005
Cycle 21 E2	1.562 +/- 0.006	1.555 +/- 0.005	1.584 +/- 0.004	1.568 +/- 0.005
Cycle 22 E1	1.564 +/- 0.006	1.557 +/- 0.005	1.585 +/- 0.003	1.571 +/- 0.005
Cycle 22 E2	1.566 +/- 0.006	1.560 +/- 0.005	1.589 +/- 0.004	1.574 +/- 0.005
Cycle 23 E1	1.566 +/- 0.006	1.561 +/- 0.005	1.589 +/- 0.004	1.573 +/- 0.005
Cycle 23 E2	1.570 +/- 0.007	1.563 +/- 0.006	1.591 +/- 0.004	1.576 +/- 0.005
Cycle 24 E1	1.569 +/- 0.006	1.562 +/- 0.005	1.591 +/- 0.004	1.576 +/- 0.005
Cycle 24 E2	1.569 +/- 0.006	1.562 +/- 0.004	1.590 +/- 0.003	1.577 +/- 0.005
Cycle 25 E1	1.571 +/- 0.006	1.565 +/- 0.004	1.594 +/- 0.004	1.579 +/- 0.005
Cycle 25 E2	1.572 +/- 0.006	1.566 +/- 0.005	1.595 +/- 0.004	1.579 +/- 0.004
Cycle 26 E1	1.576 +/- 0.006	1.569 +/- 0.005	1.597 +/- 0.004	1.581 +/- 0.005
Cycle 26 E2	1.577 +/- 0.006	1.570 +/- 0.005	1.598 +/- 0.004	1.583 +/- 0.006
Cycle 27 E1	1.578 +/- 0.007	1.572 +/- 0.005	1.600 +/- 0.004	1.585 +/- 0.006
Cycle 27 E2	1.579 +/- 0.006	1.575 +/- 0.005	1.601 +/- 0.005	1.586 +/- 0.006
Cycle 28 E1	1.582 +/- 0.006	1.574 +/- 0.005	1.604 +/- 0.004	1.589 +/- 0.005
Cycle 28 E2	1.580 +/- 0.006	1.573 +/- 0.004	1.602 +/- 0.004	1.586 +/- 0.004
Cycle 29 E1	1.584 +/- 0.006	1.577 +/- 0.004	1.605 +/- 0.003	1.590 +/- 0.005
Cycle 29 E2	1.587 +/- 0.006	1.578 +/- 0.004	1.607 +/- 0.004	1.592 +/- 0.005

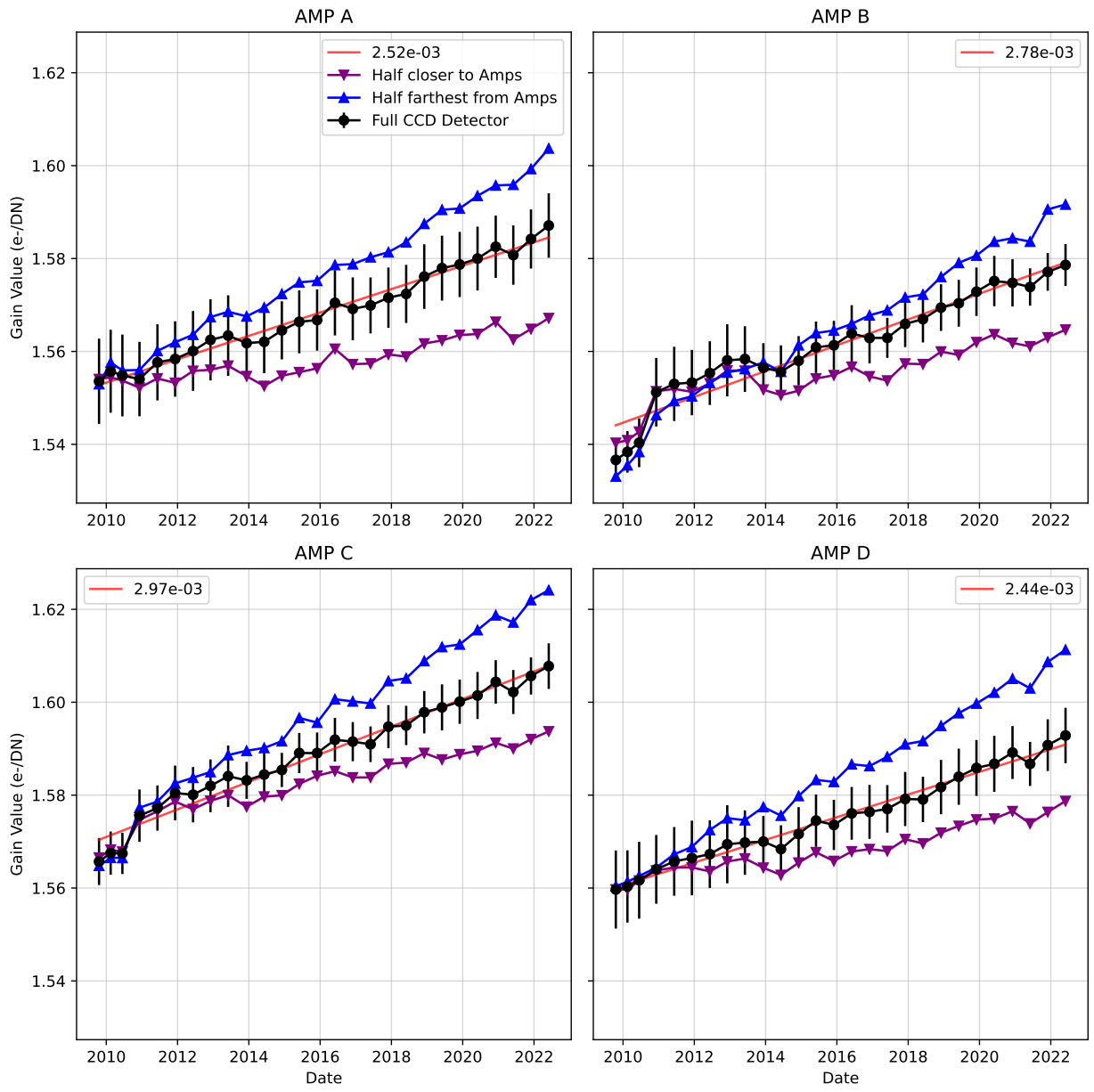

Figure 3: *Absolute gain measurements across all four amplifiers for all on-orbit data from October 2009 to June 2022 (Cycles 17 - 29) with half CCD gain values to measure CTE effects. The CCD is split into two halves horizontally, and the absolute gain is calculated for each half for a given amplifier. The upright blue triangle points represent the half that is further from the amplifier, while the upside down purple triangle points represent the half that is closer to the amplifier. Absolute gain measurements for the half closer to its respective amplifier have values that are more consistent with initial TV3 testing and early values, while gain measurements for the half further from its respective amplifier have values that are larger than the gain measurements for the full CCD detector, suggesting that CTE degradation partially affects our measurement of the gain over time.*

The gain measurements for the half of the CCD closer to the amplifiers have values that are more consistent with the initial TV3 testing and early values. Conversely, gain measurements for the half further from the amplifiers exhibit gain values that are larger than the full CCD detector, and much less agreeable with early gain values. The results from this test suggest that diminishing CTE does play a role in the increase of gain measurement over time.

Conclusions

WFC3 UVIS absolute gain measurements were made on data collected from December 2018 to June 2022 (Cycles 26 - 29) using the mean-variance technique on internal flat field image pairs taken in unbinned, 2×2, and 3×3 binned modes. We find that the latest gain values for unbinned data measured in June 2022 to be 1.587 ± 0.007, 1.578 ± 0.004, 1.607 ± 0.005, 1.592 ± 0.006 e-/DN for amps A, B, C, and D respectively. When compared to previously captured gain measurements, the gain is continuously increasing over time, however they remain within 1-2% of the initial TV3 testing. We also find that CTE degradation of the CCD detectors partially affects our measurement of the gain over time, as we observe that gain measurements made with pixels closer to the readout amplifier have values more consistent with initial TV3 testing and early measurements compared to pixels further from the readout amplifier. Gain measurement will continue to be monitored each HST Cycle for any changes in behavior that may affect the detector's health.

Acknowledgements

Many thanks Sylvia Baggett for her contribution and guidance throughout the analysis. We also thank Aidan Pidgeon and Joel Green for their thoughtful and thorough review and feedback for this report.

References

Baggett, S. (June 2008). *WFC3 TV3 Testing: UVIS-1' Gain Results.* Instrument Science Report WFC3 2008-13, 7 pages.

Fowler, J. (Oct. 2018). *WFC3/UVIS Gain Stability Results for Cycles 24 and 25.* Instrument Science Report WFC3 2018-17, 24 pages.

Gunning, Heather (Apr. 2015). *WFC3 Cycle 21 Proposal 13561: UVIS Gain.* Instrument Science Report WFC3 2015-05, 15 pages.

Martlin, C. (July 2016). *WFC3 Cycle 23 Proposal 14373: UVIS Gain.* Instrument Science Report WFC3 2016-13, 15 pages.

Appendix

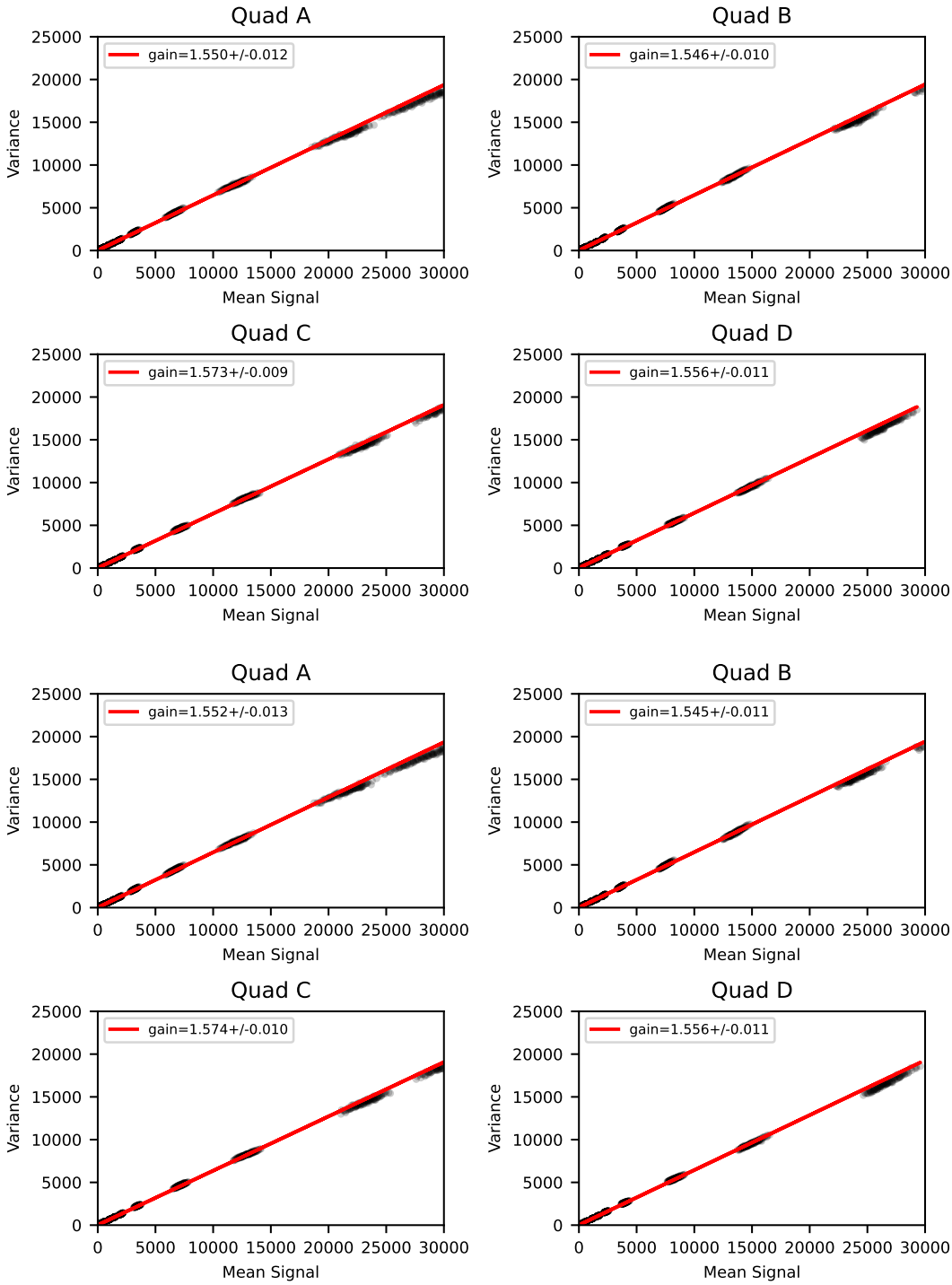

Figure 4: *Mean-variance plots for Cycle 29 unbinned CTE corrected images for Epoch 1 (Top) and Epoch 2 (Bottom) where the mean is in units of DN and the variance is in units of DN^2. The fitted slope is over plotted in red and the gain listed is the inverse slope. Each point in the plots represents the mean-variance for a square region of the detector.*

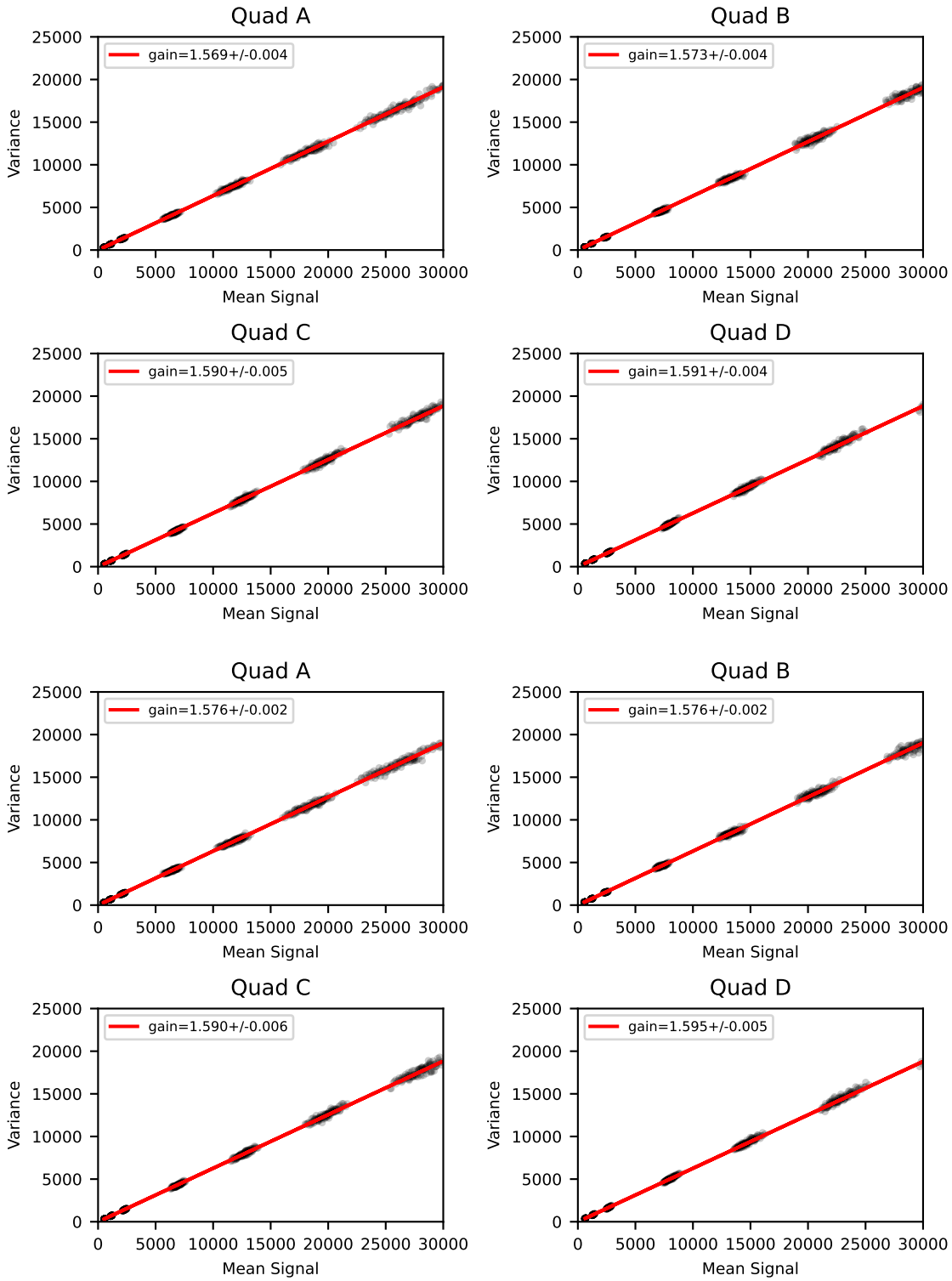

Figure 5: *Mean-variance plots for Cycle 29 2×2 binned images for Epoch 1 (Top) and Epoch 2 (Bottom) where the mean is in units of DN and the variance is in units of DN^2. The fitted slope is over plotted in red and the gain listed is the inverse slope. Each point in the plots represents the mean-variance for a square region of the detector.*

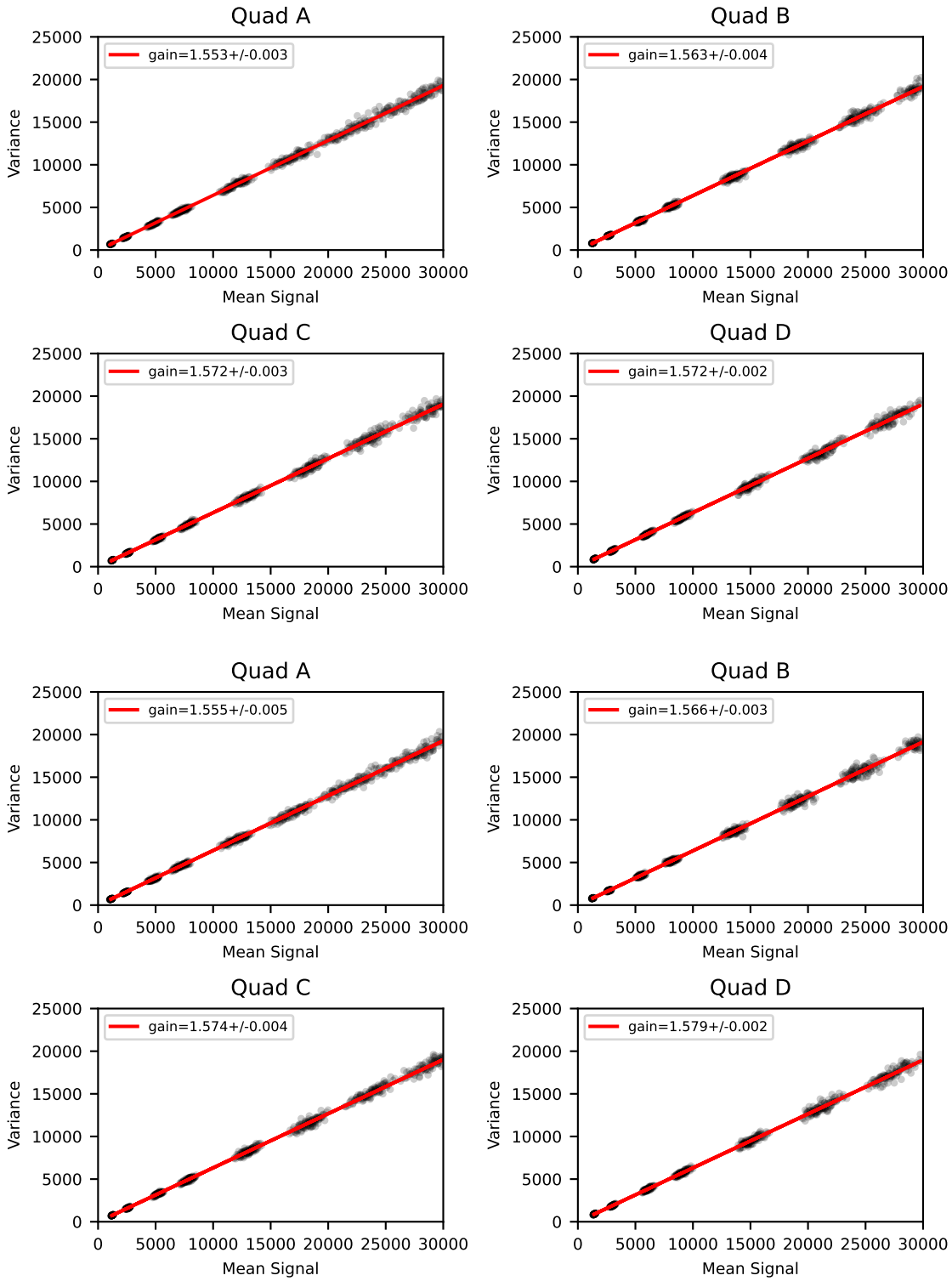

Figure 6: *Mean-variance plots for Cycle 29 3×3 binned images for Epoch 1 (Top) and Epoch 2 (Bottom) where the mean is in units of DN and the variance is in units of DN^2. The fitted slope is over plotted in red and the gain listed is the inverse slope. Each point in the plots represents the mean-variance for a square region of the detector.*

Table 2: *Proposal IDs, Cycle numbers, epochs, and binning distribution of new gain measurement dataset that were analyzed.*

Proposal ID	Cycle	Epoch	Binning
15574	26	1	1,2,3
15574	26	2	1,2,3
15719	27	1	1,2,3
15719	27	2	1,2,3
16399	28	1	1,2,3
16399	28	2	1,2,3
16571	29	1	1,2,3
16571	29	2	1,2,3